

## Peptidomimetic $\beta$ -secretase inhibitors comprising a sequence of Amyloid- $\beta$ peptide for Alzheimer's disease

Helder Vila Real, Helena Coelho, João Rocha, Adelaide Fernandes, Maria Rita Ventura, Christopher David Maycock, Olga Iranzo, and Ana Luísa Simplício

*J. Med. Chem.*, **Just Accepted Manuscript** • DOI: 10.1021/acs.jmedchem.5b00658 • Publication Date (Web): 10 Jun 2015

Downloaded from <http://pubs.acs.org> on June 22, 2015

### Just Accepted

"Just Accepted" manuscripts have been peer-reviewed and accepted for publication. They are posted online prior to technical editing, formatting for publication and author proofing. The American Chemical Society provides "Just Accepted" as a free service to the research community to expedite the dissemination of scientific material as soon as possible after acceptance. "Just Accepted" manuscripts appear in full in PDF format accompanied by an HTML abstract. "Just Accepted" manuscripts have been fully peer reviewed, but should not be considered the official version of record. They are accessible to all readers and citable by the Digital Object Identifier (DOI®). "Just Accepted" is an optional service offered to authors. Therefore, the "Just Accepted" Web site may not include all articles that will be published in the journal. After a manuscript is technically edited and formatted, it will be removed from the "Just Accepted" Web site and published as an ASAP article. Note that technical editing may introduce minor changes to the manuscript text and/or graphics which could affect content, and all legal disclaimers and ethical guidelines that apply to the journal pertain. ACS cannot be held responsible for errors or consequences arising from the use of information contained in these "Just Accepted" manuscripts.



# Peptidomimetic $\beta$ -secretase inhibitors comprising a sequence of Amyloid- $\beta$ peptide for Alzheimer's disease

Helder Vila-Real <sup>1,2</sup>, Helena Coelho <sup>1,2,3</sup>, João Rocha <sup>4</sup>, Adelaide Fernandes <sup>4</sup>, M. Rita Ventura <sup>2</sup>, Christopher D. Maycock <sup>2,5</sup>, Olga Iranzo <sup>2,6</sup>, Ana L. Simplício <sup>1,2\*</sup>

<sup>1</sup> Instituto de Biologia Experimental e Tecnológica, Av. da República, Estação Agronómica Nacional, 2780-157 Oeiras, Portugal

<sup>2</sup> Instituto de Tecnologia Química e Biológica, Av. da República, Estação Agronómica Nacional, 2780-157 Oeiras, Portugal

<sup>3</sup> Faculdade de Ciências e Tecnologia da Universidade Nova de Lisboa, Quinta da Torre, Campus Universitário, 2829-516 Caparica, Portugal.

<sup>4</sup> Faculdade de Farmácia, Universidade de Lisboa, Av. Prof. Gama Pinto, 1649-003 Lisboa, Portugal.

<sup>5</sup> Faculdade de Ciências, Universidade de Lisboa, Campo Grande, 1749-016 Lisboa, Portugal.

<sup>6</sup> Present address: Institut des Sciences Moléculaires de Marseille, Aix Marseille Université, Centrale Marseille, iSm2 UMR 7313, 13397 Marseille, France.

\*Corresponding author: Ana Simplício; E-mail: [anas@itqb.unl.pt](mailto:anas@itqb.unl.pt); Telephone: +351 214469782; Address: Av. da República, Estação Agronómica Nacional 2780-157 Oeiras, Portugal.

## Abstract

Alzheimer's disease is a grave social problem in an ageing population. A major problem is the passage of drugs through the blood-brain barrier. This work tests the hypothesis that the conjugation of peptidomimetic  $\beta$ -secretase inhibitors with a fragment of Amyloid- $\beta$  peptide facilitates entrance into the Central Nervous System.

HVR-3 (compound **4**), one of the conjugation products, was found to be as potent as OM00-3, a known peptidomimetic inhibitor, four-fold more selective towards  $\beta$ -secretase 1 in relation to  $\beta$ -secretase 2 and three-fold more resistant to *in vitro* metabolization in Human serum. Its intravenous administration to mice and Wistar rats generated an active metabolite recovered from the rodent's brains.

**Keywords:** Amyloid- $\beta$  peptide, Alzheimer's disease, blood-brain barrier, Central Nervous System, HVR-3, OM00-3, peptidomimetic  $\beta$ -secretase inhibitor.

## Introduction

Alzheimer's disease (AD), a progressive neurodegenerative disease of the Central Nervous System (CNS), is generally characterized by a slow and inflexible progression of dementia associated with cognitive and memory decline, speech loss and personality changes. Its hallmark pathological lesions occur in the brain memory and cognition regions, consisting on neurofibrillary tangles and amyloid plaques.<sup>1</sup> These plaques are composed of Amyloid- $\beta$  peptide ( $A\beta$ ), a highly insoluble peptide with tendency to oligomerize and aggregate, which is produced from the sequential cleavage of the Amyloid- $\beta$  precursor protein (APP) by  $\beta$ -secretase 1 (BACE-1) and  $\gamma$ -secretase.<sup>2</sup> In addition, neurofibrillary tangles, which are formed by the accumulation of abnormal filaments of tau protein, have been reported to be induced by  $A\beta$ , through a mechanism of hyperphosphorylation, an initiating step for tangles occurrence.<sup>3</sup> Considering this, agents capable of reducing the production of  $A\beta$ , such as BACE-1 inhibitors, may block or reduce the occurrence of amyloid plaques and neurofibrillary tangles and consequently preventing AD progression.<sup>4</sup> The first reported BACE-1 inhibitors were peptidomimetics composed of a transition-state analogue at the scissile peptide bond.<sup>5-7</sup> The Tang and Ghosh group developed compound **1** (OM00-3) (Figure 1),<sup>6</sup> one of the yet most potent BACE-1 inhibitors reported and only composed of natural amino acids plus a synthetic hydroxyethylene Leucine-Alanine dipeptide transition-state isostere. Compound **1** is an optimized compound for the inhibition of BACE-1.<sup>8</sup> Despite the high potency shown *in vitro* towards BACE-1, this kind of inhibitor has however been shown to be ineffective in the treatment of AD due to the lack of the required pharmacokinetic properties, particularly the ability to cross the blood-brain barrier (BBB). Large size and high hydrophilicity were considered the two main issues preventing passive BBB crossing and therefore attention was pointed towards the development of non-peptidic inhibitors,<sup>9,10</sup> which being smaller and more hydrophobic, have better

1  
2 conditions to permeate the BBB. Unfortunately, their therapeutic potential in the CNS has  
3  
4 been limited by P-glycoprotein efflux. Also, smaller size contributes to nonspecificity and  
5  
6 therefore to increased toxicity, contrary to peptides that are generally considered to be  
7  
8 safe. Currently there is no effective treatment capable of modifying the progression of AD  
9  
10 and available drugs only act on symptomatic improvement. The development of drugs  
11  
12 capable of blocking or delaying the disease progression remains a challenge due to the  
13  
14 inability of BACE-1 inhibitors to cross the BBB.<sup>10</sup>

15  
16  
17  
18 In this work we report a new approach to overcoming the low permeability of  
19  
20 peptidomimetic BACE-1 inhibitors across the BBB. This approach is based on the  
21  
22 conjugation of a carrier peptide with a peptidomimetic BACE-1 inhibitor in order to facilitate  
23  
24 its transcytosis across the BBB.<sup>11</sup> Compound 1 will be used as a starting compound of the  
25  
26 rational design, since it was reported to be a high potent peptidomimetic inhibitor<sup>8</sup>, but  
27  
28 simultaneously incapable to penetrate cells and to cross the plasma membrane<sup>12</sup>, being  
29  
30 widely accepted to be too large to transverse the BBB<sup>12</sup>. The transcytosis route has the  
31  
32 advantage of not limiting the compounds size for BBB permeation,<sup>12</sup> and has been targeted  
33  
34 for example through conjugation of peptidomimetic inhibitors with a fragment of Tat protein  
35  
36 from HIV-1,<sup>12</sup> as well as with the Antennapedia peptide, penetratin.<sup>13</sup>

37  
38  
39  
40  
41  
42 The innovation reported in the present work is the use of, A $\beta$  18–23', as a carrier peptide  
43  
44 for BACE-1 inhibitors through the BBB. The potential usefulness of this strategy is based  
45  
46 on the property of A $\beta$  to recognize the Receptor for Advanced Glycation Endproducts  
47  
48 (RAGE) enabling entrance into the CNS across the BBB, through receptor mediated-  
49  
50 transcytosis.<sup>14,15</sup> A $\beta$  18–23' is a hexapeptide sequence corresponding to the binding region  
51  
52 of A $\beta$  to RAGE.<sup>16</sup> Factors that may contribute for the success of using this carrier peptide in  
53  
54 AD include the following: (a) RAGE is overexpressed in AD both in the BBB and neurons,<sup>17</sup>  
55  
56  
57  
58  
59 potentially enabling a higher BBB crossing efficiency and internalization within the  
60

1  
2 endossomes of neurons, where the drug will act, through RAGE-mediated endocytosis as  
3  
4 reported for A $\beta$ ;<sup>18</sup> (b) A $\beta$  18–23' acts as a competitive inhibitor of the entry of A $\beta$  peptide  
5  
6 into cells expressing RAGE,<sup>16</sup> which potentially helps to avoid re-entry of A $\beta$  into the CNS,  
7  
8 as supported by the vascular theory for the development of AD;<sup>19</sup> (c) RAGE has  
9  
10 advantages in comparison with more ubiquitous receptors such as transferrin receptor  
11  
12 (TfR) or lipoprotein receptor-related protein (LRP) in which, competition with natural ligands  
13  
14 may contribute to adverse effects.<sup>20</sup> In the present study we specifically tested the  
15  
16 hypothesis of conjugating compound **1**,<sup>6</sup> with A $\beta$  18–23',<sup>16</sup> in order to target the CNS, thus  
17  
18 leading to a potential drug for AD treatment.  
19  
20  
21  
22  
23  
24  
25  
26  
27  
28  
29  
30  
31  
32  
33  
34  
35  
36  
37  
38  
39  
40  
41  
42  
43  
44  
45  
46  
47  
48

49 \* RAGE - Receptor for Advanced Glycation Endproducts

50  
51 TfR - transferrin receptor

52  
53 LRP - lipoprotein receptor-related protein  
54  
55  
56  
57  
58  
59  
60

## Results and discussion

The rational design of peptidomimetic BACE-1 inhibitors was based on the conjugation of **1** with A $\beta$  18–23' and on the results obtained from several tests including: BACE-1 inhibition, selectivity in relation to BACE-2, metabolization and toxicological profile and also a pharmacokinetic study in order to evaluate distribution into the brain.

### *Influence of conjugation with A $\beta$ 18–23' on BACE-1 inhibition potency*

The strategy used to design compound **2** (HVR-1) (Table 1) is outlined in Figure 1 and involved truncation of the three residue sequence at the C-terminal of **1** before conjugation with A $\beta$  18–23', in order to obtain the shortest sequence possible. This involved minimal disturbance to the original structure since the three residue sequence at the N-terminal of A $\beta$  18–23' only differs by one amino acid from the truncated sequence. This lead to a peptide of eleven residues, while the mere addition of A $\beta$  18–23' to **1** would give a sequence of fourteen residues. Therefore, the glutamic acid in position P<sub>3</sub>' of **1** becomes a phenylalanine in position 7 of **2**. This change should not affect binding to BACE-1 since the preference indexes of both residues in BACE-1 substrates are identical,<sup>8</sup> but in order to evaluate to what extent the conjugation of **1** with A $\beta$  18–23' affects the inhibition of BACE-1, compound **2** was tested for BACE-1 inhibition.

As illustrated in Figure 2, conjugation affects the potency of the inhibitor to only a very small extent ( $K_i$  (compound **2**) =  $2.0 \pm 0.1$  nM vs.  $K_i$  (compound **1**) =  $1.2 \pm 0.4$  nM, mean value  $\pm$  standard deviation,  $n = 3$ ,  $p \leq 0.05$ , independent two-tailed Student's  $t$ -test). The value reported here for the  $K_i$  of **1** is four-fold higher than the previously reported value of 0.31 nM.<sup>8</sup> This is due to the fact that a permanently active form of BACE-1 was used before, while in the present study a pro-BACE-1 was employed possessing a pro domain in equilibrium with an opened and closed form, leading to a reduction of the enzyme activity.<sup>21</sup>

1  
2 For a similar inhibitor, OM99-2, a seven-fold potency decrease was observed when pro-  
3  
4 BACE-1 ( $K_i = 9.8$  nM) was used instead of active BACE-1 ( $K_i = 1.4$  nM).<sup>21,22</sup> Moreover, the  
5  
6 potency decrease observed for **2** (about two-fold) in comparison with **1**, is less than that  
7  
8 reported for the conjugation of OM99-2 with a carrier peptide of the Tat protein of HIV-1 or  
9  
10 when **1** was conjugated with a nonapeptide of arginines, where the inhibition potency over  
11  
12 the active form of BACE-1 decreased twenty eight (39 nM) and six-fold (1.7 nM),  
13  
14 respectively, when compared to the reported value of 0.31 nM.<sup>8</sup>  
15  
16  
17  
18  
19  
20

### 21 *Effect of the exchange of a phenylalanine by a tyrosine at position 8*

22  
23 BACE-2, the closest homologous enzyme to BACE-1, has received great attention by  
24  
25 researchers due to the need to obtain a BACE-1 selective drug to avoid possible  
26  
27 secondary effects such as diabetes.<sup>23</sup> The disease may arise from BACE-2 inhibition  
28  
29 during the production of insulin by pancreatic  $\beta$ -cells.<sup>24</sup> In addition, BACE-2 contributes to  
30  
31 the degradation of  $A\beta$ ,<sup>25</sup> meaning that its inhibition may lead to the progression of AD.  
32  
33  
34

35 The results reported for the preference of amino acids at the eight subsites of BACE-1 and  
36  
37 BACE-2 substrates reveal that the preference index for phenylalanine at position  $P_4'$   
38  
39 (Figure 1) in the case of BACE-2 is very high when compared to the null preference index  
40  
41 for tyrosine,<sup>23</sup> while it is similar to the one for tyrosine in the case of BACE-1.<sup>8</sup> This means  
42  
43 that an exchange of a phenylalanine by a tyrosine in **2** should have little effect on the  
44  
45 inhibition of BACE-1 while significantly reduce affinity for BACE-2. Also, this change should  
46  
47 have minimal effect on RAGE binding since tyrosine, like phenylalanine, is a hydrophobic  
48  
49 aromatic amino acid, which is a requisite for RAGE binding. Gospodarska *et al.* reported  
50  
51 that the  $A\beta$  18–23' sequence involving a hydrophobic stretch, flanked by two negatively  
52  
53 charged residues at the C-terminal is crucial for RAGE recognition.<sup>16</sup> Based on these facts,  
54  
55 we hypothesised that the exchange of the phenylalanine for a tyrosine at position  $P_4'$ ,  
56  
57  
58  
59  
60

1  
2 corresponding to position 8 of **2**, affording compound **3** (HVR-2) (Table 1) should increase  
3  
4 the selectivity for BACE-1 in relation to BACE-2.

5  
6 As outlined in Figure 3, compound **3** shows a ratio between  $K_i^{\text{app}}_{\text{BACE-2}}$  and  $K_i_{\text{BACE-1}}$  of 7.5,  
7  
8 which is higher than that of **2** (3.7) and of **1** (2.5). The design of **3** lead therefore to an  
9  
10 inhibitor two-fold more selective than **2**, which in its turn was already more selective than **1**,  
11  
12 indicating that conjugation with the carrier peptide also contributes to increase the  
13  
14 selectivity for BACE-1 in relation to BACE-2.  
15  
16  
17  
18  
19

### 20 21 *Influence of N-terminal acylation on the metabolization profile*

22  
23 *N*-Acylation and *C*-amidation are regularly used in nature to obtain end-protected  
24  
25 neuropeptides with improved stability and activity.<sup>26</sup> Small L-amino acid peptides with free  
26  
27 *N*- and *C*-terminals suffer fast metabolization by exopeptidases, sometimes within a few  
28  
29 minutes as in the case of somatostatin, but its half-life was improved from 3 to 400 min  
30  
31 after *N*-terminal acylation.<sup>27</sup> Also, *N*-terminal acylation may improve the cell penetration  
32  
33 and passage through barriers such as the BBB due to increased lipophilicity.<sup>26</sup> Considering  
34  
35 this in order to increase the inhibitor resistance against metabolization, **3** was acetylated at  
36  
37 the *N*-terminal rendering compound **4** (HVR-3) (Table 1).  
38  
39  
40  
41

42  
43 A comparative metabolic stability study of **1**, **3** and **4** was carried out through *in vitro*  
44  
45 incubation in Human serum and mice brain homogenate. Half-lives were determined from  
46  
47 the exponential metabolization profiles shown in Figure 4. *N*-acylation contributed  
48  
49 significantly to stability as the half-lives of **4** increased three-fold in serum and two-fold in  
50  
51 brain homogenate, compared to those of **3**. The carrier peptide A $\beta$  18–23' caused however  
52  
53 some detrimental effect in the stability of **1** in brain homogenate since **1** is two-fold more  
54  
55 stable than **3**. The metabolization half-lives of **4** in serum (6.0 hours) and brain  
56  
57 homogenate (3.4 hours) indicate potential for its use as a drug. Some previously reported  
58  
59  
60

1 peptides tested for the treatment of Alzheimer's disease only last a few minutes in mice  
2  
3 brain homogenate even after *N*-terminal protection.<sup>28</sup>  
4  
5

6 The potency of **4** over BACE-1 is not statistically different from that of **1** having a  $K_i$  of  $2.0 \pm$   
7  
8  
9  
10  
11  
12  
13  
14  
15  
16  
17  
18  
19  
20  
21  
22  
23  
24  
25  
26  
27  
28  
29  
30  
31  
32  
33  
34  
35  
36  
37  
38  
39  
40  
41  
42  
43  
44  
45  
46  
47  
48  
49  
50  
51  
52  
53  
54  
55  
56  
57  
58  
59  
60  
The potency of **4** over BACE-1 is not statistically different from that of **1** having a  $K_i$  of  $2.0 \pm$   
0.6 (mean value  $\pm$  standard deviation,  $n = 3$ ,  $p > 0.05$ , independent two-tailed Student's *t*-  
test). Finally, among the studied compounds, **4** was also the most selective for BACE-1 in  
relation to BACE-2 showing a ratio of 9.2 between  $K_i^{\text{app}}_{\text{BACE-2}}$  and  $K_i_{\text{BACE-1}}$  (Figure 3), being  
four-fold more selective than **1**.

#### *Evaluation of the cytotoxic potential in Caco-2 cells*

Caco-2 cells were used as a preliminary assay to study compounds toxicity.<sup>29</sup> The  
cytotoxicity assay evaluated the dependence of Caco-2 cell viability with the inhibitor  
concentration, of compounds: **1**, **2**, **3** and **4** during incubation periods of 4 and 24 hours.  
Cellular viability was maintained above 80% within a range of 25 nM to 50  $\mu\text{M}$  for all  
inhibitors, even after 24 hours demonstrating that the compounds are not toxic up to a  
concentration magnitude that exceeds their inhibition constant of more than 25 thousand  
fold.

#### *In vivo pharmacokinetic study for evaluation of compound 4 delivery into brain*

An *in vivo* pharmacokinetic study was performed in order to evaluate the capacity of the  
best inhibitor *in vitro*, compound **4**, to reach the brain in mice. Both serum and brain  
samples were analyzed after intravenous administration of **4**. In serum samples, compound  
**4** was not detected by HPLC-FLU half an hour after intravenous administration. This  
indicates that **4** is rapidly distributed, metabolized or eliminated in mice. Accordingly,  
compound **4** with a peak of 1326.5 amu and a retention time of 23.6 minutes could not be  
detected in brain samples; however, a metabolite with a peak of 1285.4 amu (Figure 5) and

1  
2 a very close retention time of 22.9 minutes was detected in brain samples by HPLC-FLU  
3  
4 and LC-MS even two hours after administration. The fact that this metabolite doesn't  
5  
6 appear in serum samples dismisses any potential contamination of brain samples by the  
7  
8 blood.  
9

10  
11 In order to identify the metabolite and according to the mass found it was hypothesized that  
12  
13 it could be compound **5** (HVR-4) (table 1) as the molecular ion found (1285.4 amu) is  
14  
15 consistent with the calculated exact mass for **5**  $[M+H]^+$  (1285.6 amu). The MS<sup>2</sup>  
16  
17 fragmentation of the molecular ion: 1285.4 amu, afforded the fragmentation spectrum  
18  
19 shown in Figure 5 and the main  $m/z$  peaks were assigned based on the expected ions  
20  
21 given by mMass software for compound **5**,<sup>30</sup>: M-H<sub>2</sub>O (expected = 1267.6, found = 1267.4),  
22  
23 M-2H<sub>2</sub>O (expected = 1249.6, found = 1249.4), b<sub>10</sub> (expected = 1152.5, found = 1152.5),  
24  
25 z<sub>10</sub>-H<sub>2</sub>O (expected = 1121.5, found = 1121.7), b<sub>9</sub> (expected = 1023.5, found = 1023.3), b<sub>8</sub>  
26  
27 (expected = 952.4, found = 952.4), a<sub>8</sub> (expected = 924.5, found = 924.4), b<sub>7</sub> (expected =  
28  
29 789.3, found = 789.4), a<sub>7</sub>-H<sub>2</sub>O (expected = 743.4, found = 743.2), b<sub>6</sub> (expected = 642.4,  
30  
31 found = 642.4), b<sub>6</sub>-H<sub>2</sub>O (expected = 624.4, found = 624.3), z<sub>5</sub>-H<sub>2</sub>O (expected = 610.2,  
32  
33 found = 610.2) and b<sub>5</sub> (expected = 543.3, found = 543.2). The correspondence between  
34  
35 the observed  $m/z$  peaks (Figure 5) with the expected ions given by mMass suggests  
36  
37 compound **5** as the metabolite found in the brain samples.  
38  
39  
40  
41  
42  
43

44  
45 In order to further confirm the chemical structure of the metabolite as **5**, compound **3** was  
46  
47 hydrolyzed in order to generate **5** by chemical deamination of the C-terminal. The C-  
48  
49 terminal amide of **3** is the only primary amide present making it the most prone to suffer  
50  
51 hydrolysis under moderate basic conditions (Figure 6). The hydrolysis product was  
52  
53 analyzed by HPLC-FLU and LC-MS, having the some retention time of 22.9 min (Figure 7)  
54  
55 as the metabolite (Figure 5) and the major molecular ion found (1285.6 amu) (Figure 8) is  
56  
57 consistent with the calculated exact mass for **5**  $[M+H]^+$  (1285.6 amu). A final confirmation  
58  
59  
60

1  
2 of the metabolite structure was provided by the correspondence of the MS<sup>2</sup> fragmentation  
3 spectrum of the metabolite (Figure 5) with that of the product of hydrolysis (Figure 8),  
4 where all the main peaks identified in the product of hydrolysis (Figure 8) were also  
5 identified in the fragmentation spectrum of the metabolite, even including peak b10-H<sub>2</sub>O  
6 (1134.6) not highlighted in Figure 5 but still present.  
7  
8

9  
10  
11  
12  
13 In a parallel experiment used to detect **4** by MALDI-TOF/TOF in several brain regions of  
14 Wistar rats, **4** also suffered biotransformation into **5**. In agreement with previous  
15 experiments in mice, **4** was not detected in the rat cortex after two hours, but **5** was. On the  
16 other hand, both **4** and **5** were detected in serum samples of Wistar rats after two hours,  
17 raising the hypothesis that disposition of **4** is faster in mice than in Wistar rats.  
18  
19

20  
21 During the biotransformation of **4** into **5**, the peptide suffered hydrolytic reactions at both  
22 the *N*- and *C*-terminal amides. Despite being generally considered robust amine  
23 derivatives,<sup>31</sup> amides do suffer metabolization. As shown on Figure 4, **4** is in fact two-fold  
24 more stable than **5** in Human serum, possibly because the latter is more susceptible to the  
25 attack of serum exopeptidases. On the other hand the opposite happened in mice brain  
26 homogenate (Figure 4), where **5** is more stable than **4**. In the brain the action of amidases  
27 acting on terminal amides seem to be more relevant than exopeptidases. Primary amides,  
28 such as the *C*-terminal amide of **4**, are easily converted into the corresponding acid by  
29 amidases,<sup>32</sup> which are nonspecific hydrolytic enzymes mainly found in the liver.<sup>33</sup>  
30 Amidases may also be found in other organs including kidney and brain, where *N*-  
31 deacylation of acetophenetidines has been observed.<sup>34</sup>  
32  
33  
34  
35  
36  
37  
38  
39  
40  
41  
42  
43  
44  
45  
46  
47  
48  
49  
50

51 The modifications suffered by **4** when converted to **5** are slight, and resulted in an active  
52 metabolite as potent as **4** ( $1.7 \pm 0.2$  nM, mean value  $\pm$  standard deviation,  $n = 3$ ,  $p > 0.05$ ,  
53 independent two-tailed Student's *t*-test). The high potency of **5** was expected since it has a  
54 very similar structure to **3** (the only difference between **5** and **3** is in the *C*-terminal,  
55  
56  
57  
58  
59  
60

1  
2 possessing a carboxylic acid instead of an amide) that is as potent as **4**. The benefits of  
3  
4 having an amide at the C-terminal is dual, namely the increase in the resistance against  
5  
6 metabolization in serum and the absence of a negative charge that could disturb RAGE  
7  
8 binding and consequently, BBB crossing.<sup>16</sup> Since **5** was found in the brain, this means that  
9  
10 either RAGE binding is not affected or that deamidation is slow enough to allow prior  
11  
12 distribution to the brain. Moreover the presence of the carboxylic acid at the C-terminal also  
13  
14 didn't affect BACE-1 inhibition due to the long distance in relation to the binding site (Figure  
15  
16  
17  
18  
19 1).

20  
21 Looking from a different perspective, the chemical modifications induced by the  
22  
23 biotransformation of **4** can be even more important for therapy than the initial compound  
24  
25 itself. The primary amine formed at the N-terminal and the carboxylic acid at the C-terminal  
26  
27 increase the molecule hydrophilicity, by the generation of a positive and a negative charge,  
28  
29 respectively, at physiological pH. These chemical changes will contribute to impede **5**  
30  
31 clearance from the CNS into the bloodstream leading to a higher residence time in the  
32  
33 CNS since a more hydrophilic molecule will have more difficulty diffusing across the BBB  
34  
35 into the bloodstream.<sup>26</sup> This hypothesis gains even more support by the fact that **5** was  
36  
37 found at approximately 20 nM in mice brain up to one hour after administration, which is  
38  
39 within the therapeutic concentration range, while **4** was not detected after half an hour post  
40  
41  
42  
43  
44  
45  
46  
47  
48  
49  
50  
51  
52  
53  
54  
55  
56  
57  
58  
59  
60 administration.

## Conclusions

The conjugation of **1** with A $\beta$  18–23' giving compounds **2**, **3** and **4** shows little or no effect on the BACE-1 inhibition potential and at the same time contributes to increased selectivity in relation to BACE-2, with **4** exhibiting four-fold more selective than **1** for BACE-1 in relation to BACE-2. Compound **4** was also demonstrated to be more resistant against *in vitro* metabolism in Human serum (three-fold).

Preliminary data in Caco-2 cells indicates that compounds **1**, **2**, **3** and **4** are potentially non toxic in concentrations that are therapeutically relevant, which complies with the general idea of peptides being low toxicity drugs.

Compound **4** was not detected in serum, nor in mice brain after intravenous administration, but **5**, an active metabolite of **4**, was found in mice brain and Wistar rat cortex after two hours post administration. Peptide **4** suffered two biotransformation steps elicited by amidases consisting of an *N*-deacylation and a *C*-deamination. This transformation afforded an active metabolite, **5** having increased hydrophilicity that may contribute to a larger residence time in the CNS thus increasing its therapeutic index.

We conclude that the design of compound **4**, a peptidomimetic BACE-1 inhibitor based on the conjugation of **1** with A $\beta$  18–23', was successful in targeting the CNS. Altogether these results corroborate the potential of **4** to reach CNS as a prodrug for the treatment of Alzheimer's disease. Future developments include the use of AD mice models to determine the efficacy of **4** as a prodrug.

## Experimental section

### *Peptide synthesis and purification*

Peptides were synthesized by manual standard Solid Phase Peptide Synthesis procedure using standard protocols,<sup>35</sup> starting from Fmoc-protected amino acids (Novabiochem) activated with *N,N,N',N'*-Tetramethyl-O-(1H-benzotriazol-1-yl)uronium hexafluorophosphate (HBTU) and 1-hydroxybenzotriazole (HOBt) using *N,N*-diisopropylethylamine (DIEA) in dimethylformamide. A Rink amide resin (MBHA resin [100-200 mesh], 0.59 mmol/g substitution, Novabiochem) was used for peptide synthesis yielding a C-terminal amide upon resin cleavage. Exceptions were **1** and the fluorogenic product (Mca-SEVNL-COOH) of the hydrolysis of Mca-SEVNLDAEFK-DNP by BACE-1 for which two Wang resins were used to generate a C-terminal carboxylic acid instead; these were respectively: Fmoc-Phe-Wang resin ([100-200 mesh], 0.61 mmol/g substitution, Novabiochem) and Fmoc-Leu-Wang resin ([100-200 mesh], 0.64 mmol/g substitution, Novabiochem). Capping of the N-terminal was accomplished for **4** (Table 1) with 50 equivalents of acetic anhydride and 25 equivalents of DIEA in dimethylformamide during 1 hour, after Fmoc deprotection of the last added amino acid with 20% piperidine in dimethylformamide. In the synthesis of Mca-SEVNL-COOH, 7-methoxycoumarin (Mca) (Novabiochem) was added to the N-terminal of SEVNL-COOH activated by O-(7-azabenzotriazol-1-yl)-1,1,3,3-tetramethyl-uronium hexafluorophosphate (HATU) and HOBt in dimethylformamide. The Fmoc-Leu\*Ala isostere was synthesized as previously described,<sup>36</sup> and was incorporated into peptides: **1**, **2**, **3** and **4** using the same standard protocols as for natural amino acids.

Peptides were purified by preparative reverse-phase HPLC and lyophilized. Chromatographic conditions were as follow: column C12 (Jupiter Proteo, Phenomenex) 250 mm x 21.2 mm, 4 μm; eluent (A) water/TFA (99.9:0.1, V/V), (B) acetonitrile/water/TFA

1  
2 (90:9.9:0.1, V/V). The flow rate was 10 mL/min and the column was kept at room  
3  
4 temperature. Re-analysis by analytical reverse-phase HPLC and Electrospray Mass  
5  
6 Spectrometry (ESI-MS analysis) is in accordance with a homogenous product of 98% purity  
7  
8 or higher. Molecular structures and molecular masses of the synthetic peptides inhibitors of  
9  
10 BACE-1 are outlined in Table 1.  
11  
12

### 13 14 15 16 *Assay for BACE-1 and BACE-2 activities*

17  
18 The kinetic experiments were preformed in 20 mM sodium acetate buffer, pH 4.5 at 37°C in  
19  
20 15% dimethyl sulfoxide (DMSO), 1% triton X-100 (Sigma-Aldrich), 250 nM of Mca-  
21  
22 SEVNLDAEFK-DNP (Bachem) as substrate and 2 U/mL of BACE-1 (human, recombinant,  
23  
24 21267 U/mg, purity > 90%, Sigma-Aldrich) or 10 U/mL of BACE-2 (human, recombinant,  
25  
26 40000 U/mg, purity > 80%, Enzo). The initial rates of substrate hydrolysis were confirmed  
27  
28 to be directly proportional to the enzyme concentrations in a range of 1 - 5 U/mL for BACE-  
29  
30 1 and 5 - 20 U/mL for BACE-2. Initial rates were determined below conversion of 5% of  
31  
32 substrate, after stopping the reaction with 25% of a 2.5 M sodium acetate solution after 2  
33  
34 and 1 hour for BACE-1 and BACE-2, respectively. The hydrolysis of the fluorogenic  
35  
36 substrate was quantified by reverse phase HPLC with fluorescence detection (HPLC-FLU)  
37  
38 using an excitation wavelength of 323 nm and an emission wavelength of 382 nm (Merck  
39  
40 Hitachi, Elite LaChrom). A C18 column (Gemini, Phenomenex) 150 mm, 4.60 mm, 5 µm  
41  
42 was used at 30°C with a linear gradient from (A) water/TFA (99.9:0.1, V/V), to (B)  
43  
44 acetonitrile/water/TFA (90:9.9:0.1, V/V) at 1 mL/min. The program started at 90% A for two  
45  
46 min, graded to 70% A during ten min and finally to 0% A during two min. The retention time  
47  
48 of the reaction product (Mca-SEVNL-COOH) was 11 minutes and quantification was  
49  
50 performed by external calibration, using a peptide synthesized and purified as in the  
51  
52 Peptide synthesis and purification section.  
53  
54  
55  
56  
57  
58  
59  
60

### *Determination of apparent tight-binding inhibition constants*

Apparent tight-binding inhibition constants,  $K_i^{\text{app}}$ , were determined from the fitting of experimental dose-response data to the Morrison equation (Equation 1), where  $v$  is the initial rate observed at each inhibitor concentration,  $[I]$ ,  $v_0$  is the initial rate observed without inhibitor and  $[E]$  is the enzyme concentration.<sup>37,38</sup> Enzyme as well as substrate concentrations were kept constant with increasing inhibitor concentration, ranging from 0.04 nM to 283 nM, according to the potency of the inhibitor. The Morrison equation fit to experimental data was carried out through non-linear regression by minimising the residual sum of squares between the experimental data points of the relative activity vs the logarithm of the inhibitor concentration and those estimated by the model, using Solver add-in from Microsoft Excel 2003, considering the following options: Newton method; 100 iterations, precision of  $10^{-6}$ , 5 % of tolerance and  $1 \times 10^{-4}$  convergence.

$$v = v_0 \frac{[E] - [I] - K_i^{\text{app}} + \sqrt{([E] - [I] - K_i^{\text{app}})^2 + 4[E]K_i^{\text{app}}}}{2[E]}$$

**Equation 1**

### *Determination of the inhibition constants for BACE-1*

Inhibition constants,  $K_i$ , were determined for BACE-1, from the direct application of the Cheng-Prusoff equation (Equation 2),<sup>39</sup> and using the  $K_M$  value reported of 4.5  $\mu\text{M}$  for the Mca-SEVNLDAEFK-DNP substrate.<sup>21</sup> For BACE-2, the  $K_M$  has not yet been reported and therefore  $K_i$  was not determined.

$$K_i = \frac{K_i^{\text{app}}}{\left[1 + \frac{[S]}{K_M}\right]}$$

**Equation 2**

### *In vitro metabolic stability assay*

Compounds were prepared at 50  $\mu\text{M}$  in phosphate-buffered saline (PBS) with 2% DMSO. 10  $\mu\text{L}$  of the solution was added to of Human serum (40  $\mu\text{L}$ ) or to 10% of mice brain homogenate in PBS with 0.5% Triton X-100 (40  $\mu\text{L}$ ). All compounds were tested using the same biological samples of Human serum and mice brain homogenate to assure identical deactivation conditions. The solutions were incubated during different time periods at 37°C, after which metabolization was stopped by adding one volume of acetonitrile. Precipitated serum and brain proteins were removed by centrifugation at 14000  $g$  for 10 min. Tests were made confirming that acetonitrile does not precipitate the synthetic peptides. The remaining peptide in the supernatant was quantified by HPLC-FLU (Merck Hitachi, Elite LaChrom), ( $\text{ex}_\lambda = 255 \text{ nm}$  and  $\text{em}_\lambda = 285 \text{ nm}$ , to detect compounds containing phenylalanine, and  $\text{ex}_\lambda = 275 \text{ nm}$  and  $\text{em}_\lambda = 307 \text{ nm}$  whenever tyrosine is present). Chromatographic conditions were as described for determination of enzyme activities. A calibration curve was built for each compound and the decay in the concentration of the peptide in the incubated samples was followed till approximately 50% decay.

The metabolization kinetics of the synthetic peptides followed a monophasic behavior in vitro. The fit of a monophasic deactivation model to experimental data was carried out through non-linear regression by minimising the residual sum of squares between the experimental data points of the relative quantity of intact product vs. time and those estimated by the model, using Solver add-in from Microsoft Excel 2003, considering the following options: Newton method; 100 iterations, precision of  $10^{-6}$ , 5 % of tolerance and  $1 \times 10^{-4}$  convergence. The half-life,  $t_{1/2}$ , was determined trough interpolation.

### *Cytotoxicity assay*

1  
2 Human colon carcinoma cells (Caco-2) from the *American Type Culture Collection* (ATCC  
3 HTB-37), between passage number 26 to 41, were routinely cultured in T-75 flasks (BD  
4 Biosciences) using high glucose (4.5 g/L) Dulbecco's Modified Eagle Medium (DMEM),  
5  
6 supplemented with 10% (v/v) fetal bovine serum (FBS) and 1% (v/v) non-essential  
7  
8 aminoacids (Gibco; Grand Island, USA), at 37 °C in a humidified atmosphere containing  
9  
10 5% (v/v) CO<sub>2</sub>. Once a week, before reaching confluence, cells were cultured using  
11  
12 Dulbecco's phosphate buffered saline (DPBS) and 0.25% (w/v) Trypsin-EDTA (Gibco). The  
13  
14 cytotoxicity assay was performed using the Promega CellTiter 96 cellular viability assay,  
15  
16 MTS, to determine the number of viable cells in culture. Confluent Caco-2 cells were  
17  
18 incubated with increasing concentrations of testing compounds from 2.5 nM to 50 μM in 0.5  
19  
20 % FBS supplemented DMEM, for 4 hours and 24 hours exposure periods. After the  
21  
22 incubation period the medium was removed and 100 μL of MTS mixture was added to  
23  
24 each well. Cells were incubated with MTS for 4 hours at 37°C with 5% CO<sub>2</sub> at fully  
25  
26 humidified atmosphere. After the incubation period the absorbance of formazan was read  
27  
28 at 490 nm using a plate reader (BioTek™ Power Wave XS). The results were determined  
29  
30 as a percentage of the cellular viability in relation to the control composed of cells with  
31  
32 0.5% FBS supplemented DMEM.  
33  
34  
35  
36  
37  
38  
39  
40  
41  
42  
43  
44

#### 45 *Distribution study in animals*

46  
47 Female mice (n = 12, 8 – 12 weeks, weighing 22 – 37 g) and male Wistar rats (n = 8, 8 –  
48  
49 12 weeks, weighing 182 – 201 g) were purchased from Harlan Ibérica, Barcelona, Spain.  
50  
51 All animals received a standard diet and water ad libitum. Experiments were conducted  
52  
53 according to the Home Office Guidance in the Operation of Animals (Scientific Procedures)  
54  
55 Act 1986, published by Her Majesty's Stationary Office, London, UK and the Institutional  
56  
57  
58  
59  
60

1  
2 Animal Research Committee Guide for the Care and Use of Laboratory Animals published  
3  
4 by the US National Institutes of Health (NIH Publication No. 85-23, revised 1996), as well  
5  
6 as to the currently adopted EC regulations (2010/63/EU). Finally, the studies are in  
7  
8 compliance with the ARRIVE Guidelines for Reporting Animal Research' summarized at  
9  
10 [www.nc3rs.org.uk](http://www.nc3rs.org.uk). Before experiments animals were fasted for 24h.  
11  
12

13  
14 PBS was used to prepare a solution of **4** for intravenous administration at a dose of 0.53  
15  
16 mg/kg. Experiments were done in triplicate. Mice and Wistar rats were sacrificed at 0.5, 1  
17  
18 and 2 hours after dosing and were previously anesthetized with sodium pentobarbital (6  
19  
20 mg/kg i.p.) for collection of blood by cardiac puncture and brain tissue was perfused by  
21  
22 intraventricular injection of 10 mL of chilled saline solution to remove residual blood.  
23  
24  
25

### 26 27 28 *Animal samples preparation*

29  
30 Serum was isolated from the blood samples by centrifugation at 657 g for 10 min, at 4°C.  
31  
32 Serum proteins were precipitated with one volume of acetonitrile and were removed by  
33  
34 centrifugation at 14000 g for 10 min. Brain was promptly removed and washed with PBS  
35  
36 and blotted dry. Meninges were carefully removed. In the case of Wistar rats only cortex  
37  
38 and hippocampus were collected while for mice the whole brain was used. The brain  
39  
40 samples were homogenized with 2 volumes (V/w) of PBS/acetonitrile/Triton X-100  
41  
42 (50/50/0.5) using firstly a pestle and then a pipette and finally a sonicator. Compound **3**  
43  
44 was added as internal standard to best mimic the recovery of compound **4**. The pellet was  
45  
46 removed centrifuging at 14000 g for 10 min. Samples were purified by preparative reverse-  
47  
48 phase HPLC Using a C18 column (Jupiter, Phenomenex) 250 x 21.2 mm, 5 µm.  
49  
50 Chromatographic conditions were as follow: eluent (A) water/TFA (99.9:0.1, V/V), (B)  
51  
52 acetonitrile/water/TFA (90:9.9:0.1, V/V). The linear gradient was started at 80 % A, graded  
53  
54 to 68% for 2 min and then was kept at 68% for 17 min finally grading to 0% A for 5 min.  
55  
56  
57  
58  
59  
60

1  
2 The flow rate was 10 mL/min and the column was at room temperature. Collected fractions  
3  
4 (100 ml) were lyophilized, reconstituted in 200  $\mu$ L of PBS and stored at  $-20^{\circ}\text{C}$  prior  
5  
6 analysis.  
7  
8

### 9 10 11 *Analysis of animal samples*

12  
13 Mice samples were analyzed for detection of the compounds (**4** and their metabolites) by  
14  
15 HPLC-FLU using an excitation wavelength of 275 nm and an emission wavelength of 307  
16  
17 nm, as well as by LC-ESI-MS (LTQ, ThermoFinnigan) in the positive mode. Mass range was  
18  
19 measured from 250-2000 amu. The ESI source conditions were adjusted as follows:  
20  
21 source capillary operating at 5 kV and source temperature at  $300^{\circ}\text{C}$ . A full-scan MS  
22  
23 method in positive mode was used for sample analysis of the molecular ions:  $[\text{M}+\text{H}]^{+}$ ,  
24  
25  $[\text{M}+\text{Na}]^{+}$  of **4** as well as its metabolites. The chromatographic step was performed in a C8  
26  
27 column (LiChroCART, Merck) 100 mm x 4.6 mm, 5  $\mu\text{m}$  at  $30^{\circ}\text{C}$  and 1 mL/min, under the  
28  
29 following conditions: eluent (A) water/formic acid (99.9:0.1, V/V), (B)  
30  
31 acetonitrile/water/formic acid (90:9.9:0.1, V/V). Water and acetonitrile were of LC-MS  
32  
33 grade. The linear gradient was initially at 80 % A and graded to 65 % eluent A during 27  
34  
35 min, and to 0 % eluent A for another minute.  
36  
37  
38  
39  
40  
41

42 For identification of **4** and its metabolite in Wistar rat brain, samples were analysed using a  
43  
44 4800plus MALDI-TOF/TOF (AB Sciex) mass spectrometer in the positive reflector MS and  
45  
46 MS/MS modes with 3200 laser shots per spectrum and data was collected using the 4000  
47  
48 Series Explorer Software v.3.5.3 (Applied Biosystems). The maximum precursor mass  
49  
50 tolerance (MS) was 50 ppm and the maximum fragment mass tolerance (MS/MS) was 0.3  
51  
52 Da. 0.6  $\mu\text{L}$  of each sample was directly spotted on a MALDI plate and 0.6  $\mu\text{L}$   $\alpha$ -Cyano-4-  
53  
54 hydroxycinnamic acid (CHCA) matrix (LaserBio Labs; 5mg/ml in 50% (V/V) acetonitrile with  
55  
56 5% (v/v) formic acid) was added.  
57  
58  
59  
60

1  
2 For confirmation purposes of the metabolite found *in vivo*, **5** was produced from **3**: 200  $\mu$ M  
3  
4 of **3** were hydrolyzed in a 500 mM aqueous solution of Sodium Hydroxide overnight.  
5  
6 Reaction was stopped at pH = 7 with acetic acid and the product **5** was obtained in a 52%  
7  
8 yield after purification by preparative reverse-phase HPLC and lyophilization, using the  
9  
10 chromatographic conditions previously described for peptides. Re-analysis by analytical  
11  
12 reverse-phase HPLC-UV, LC-MS, MS/MS and MALDI-TOF/TOF is in accordance with a  
13  
14 homogenous product. The molecular structure and molecular mass of the product of  
15  
16 hydrolysis **5** is outlined in Table 1.  
17  
18  
19  
20  
21  
22

23 \*HBTU - *N,N,N',N'*-Tetramethyl-O-(1H-benzotriazol-1-yl)uronium hexafluorophosphate

24  
25  
26 HOBt - 1-hydroxybenzotriazole

27  
28 DIEA - *N,N*-diisopropylethylamine

29  
30 Mca - 7-methoxycoumarin

31  
32  
33 DNP - 2,4-dinitrophenol

34  
35  
36 FLU - Fluorescence

37  
38  $K_i^{app}$  - Apparent tight-binding inhibition constants

39  
40 DMEM - Dulbecco's Modified Eagle Medium

41  
42 FBS - fetal bovine serum

43  
44  
45 DPBS - Dulbecco's phosphate buffered saline

46  
47 MTS - 3-(4,5-dimethylthiazol-2-yl)-5-(3-carboxymethoxyphenyl)-2-(4-sulfophenyl)-2H-  
48  
49 tetrazolium

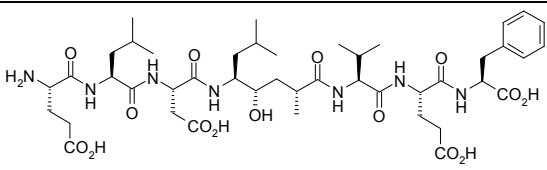
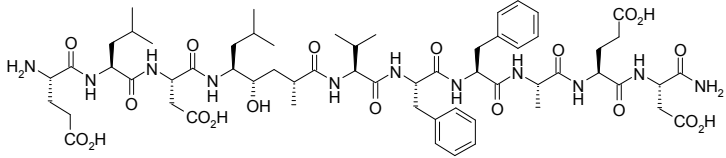
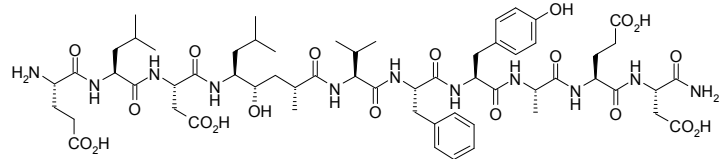
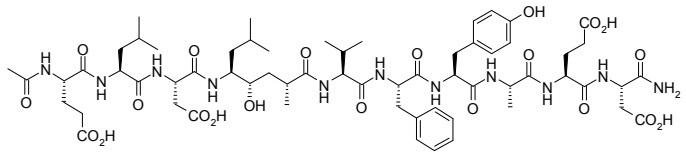
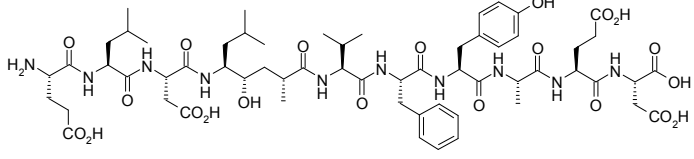
50  
51  
52 CHCA -  $\alpha$ -Cyano-4-hydroxycinnamic acid  
53  
54  
55  
56  
57  
58  
59  
60

## Acknowledgements

We wish to acknowledge the financial support provided by Fundação para a Ciência e a Tecnologia through the Strategic Project: PEst-OE/EQB/LA0004/2013, the Postdoc grant SFRH/BPD/82097/2011 and its support for the NMR spectrometers as part of The National NMR Facility (RECI/BBB-BQB/0230/2012) and the mass spectrometers as part of the *Rede Nacional de Espectrometria da Massa* (RNEM). We also would like to acknowledge the UniMS – Mass Spectrometry Unit and particularly Elisabete Pires, ITQB/IBET (Oeiras, Portugal) for mass spectrometry analysis. Finally, we also acknowledge Liliana Bernardino and Ana Clara Cristovão from UBI (Covilhã, Portugal), for their proactive help in the tests using Wistar rats.

## Tables

Table 1:

#	Structure	M.M. / g.mol <sup>-1</sup> (exact mass / amu)	K <sub>i</sub> BACE-1 / nM	K <sub>i</sub> <sup>app</sup> BACE-2 / nM	K <sub>i</sub> <sup>app</sup> BACE-2 · K <sub>i</sub> BACE-1 <sup>-1</sup>
1		936.1 (935.5)	1.2 ± 0.4	3.0 ± 0.3	2.5
2		1268.4 (1267.6)	2.0 ± 0.1	7.3 ± 0.9	3.7
3		1284.4 (1283.6)	1.9 ± 0.2	14.2 ± 2.2	7.5
4		1326.5 (1325.6)	2.0 ± 0.6	18.3 ± 0.5	9.2
5		1285.4 (1284.6)	1.7 ± 0.2	12.7 ± 1.9	7.5

## Figures

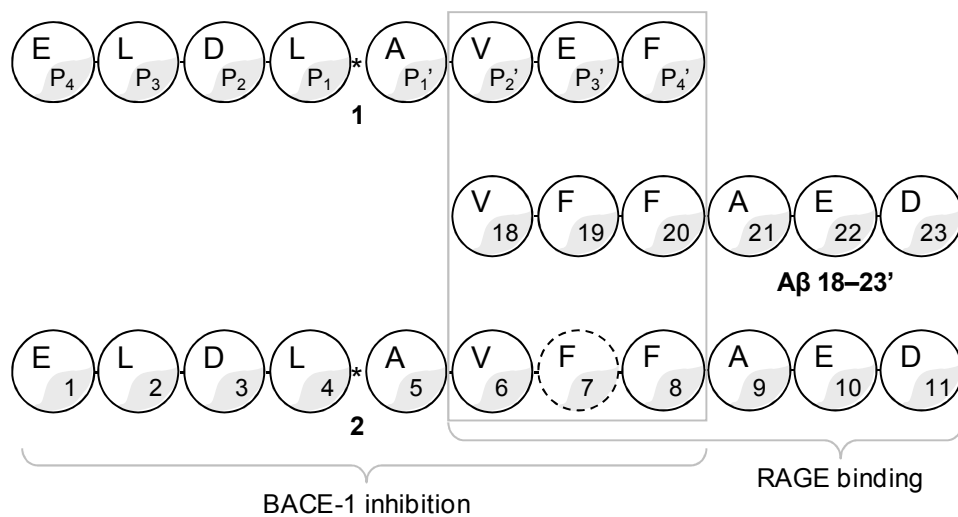


Figure 1:

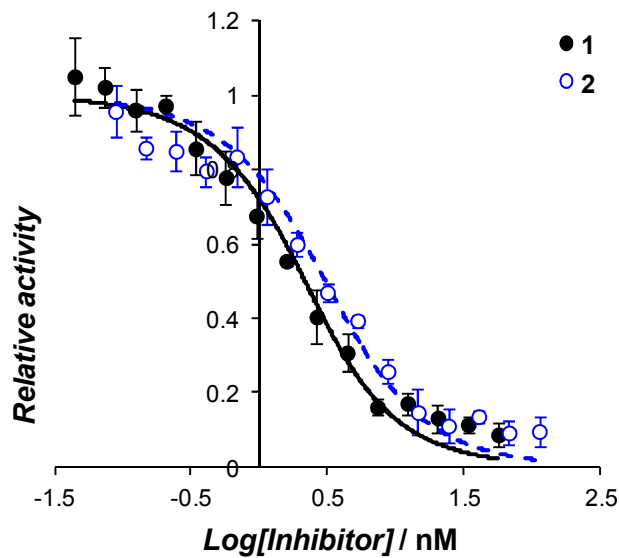


Figure 2:

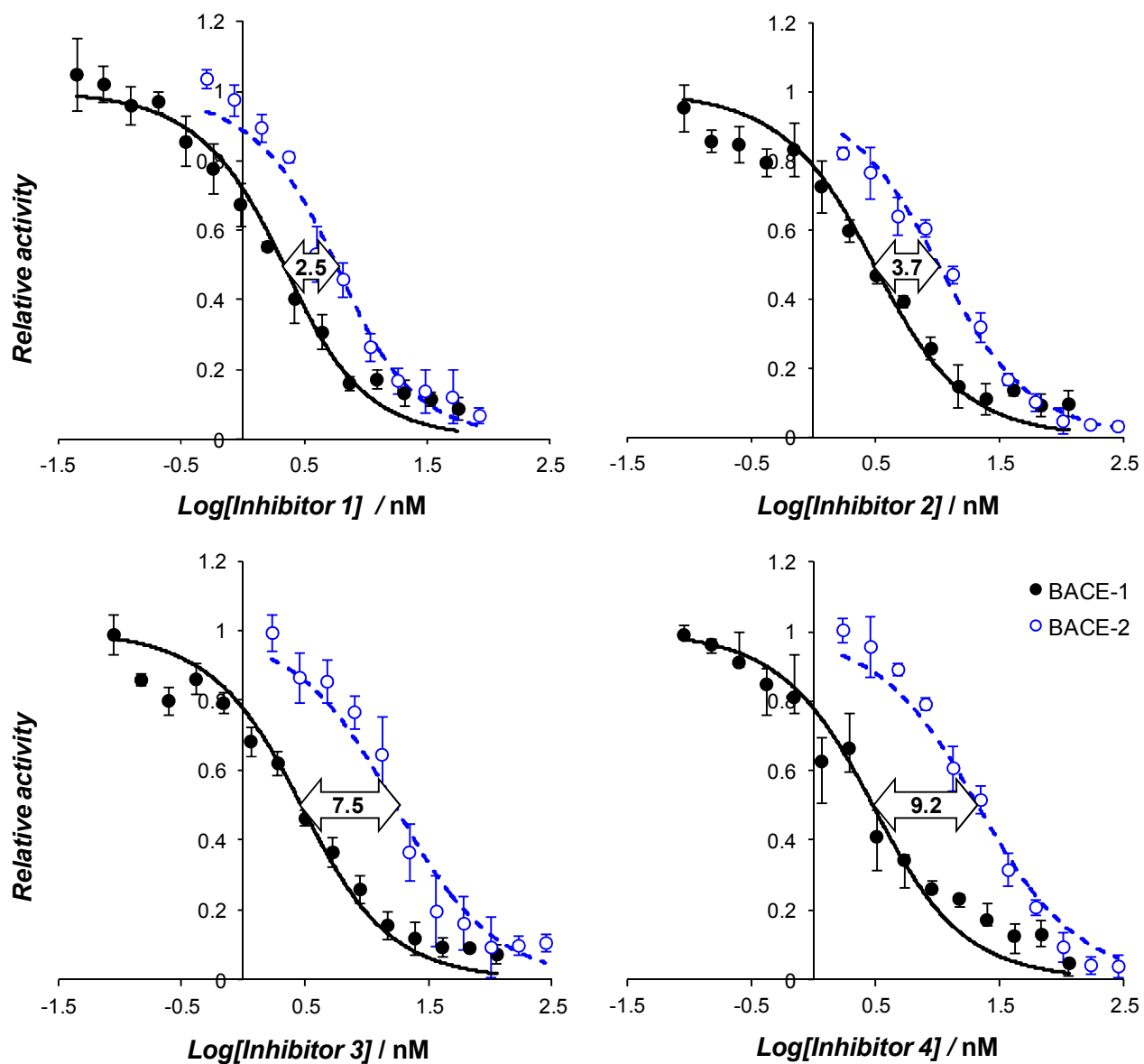


Figure 3:

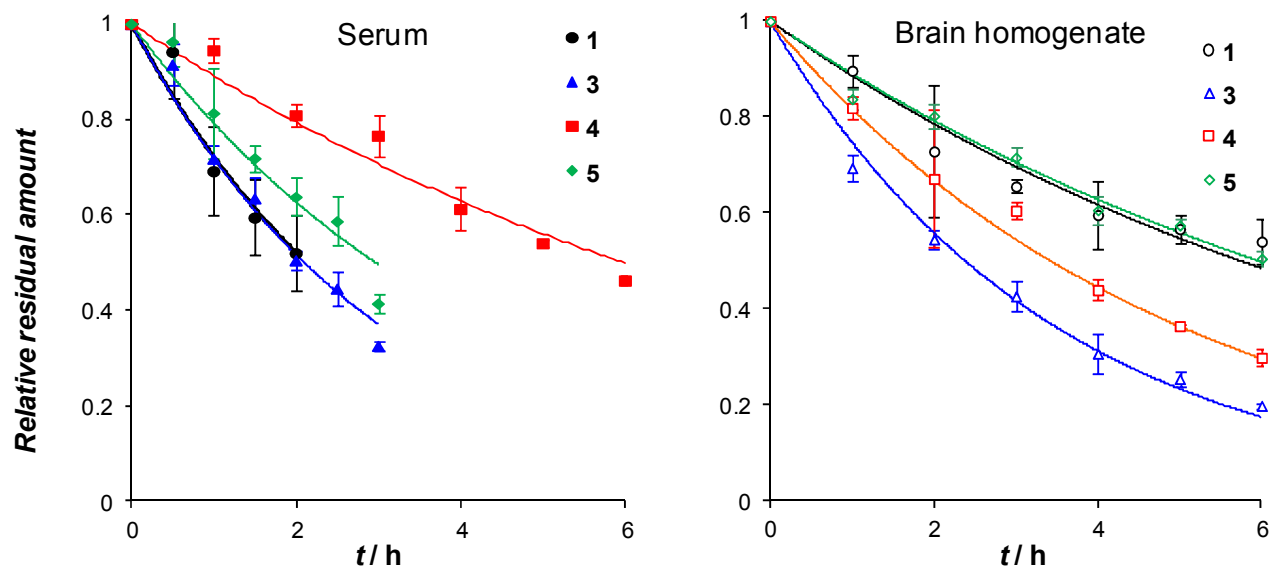


Figure 4:

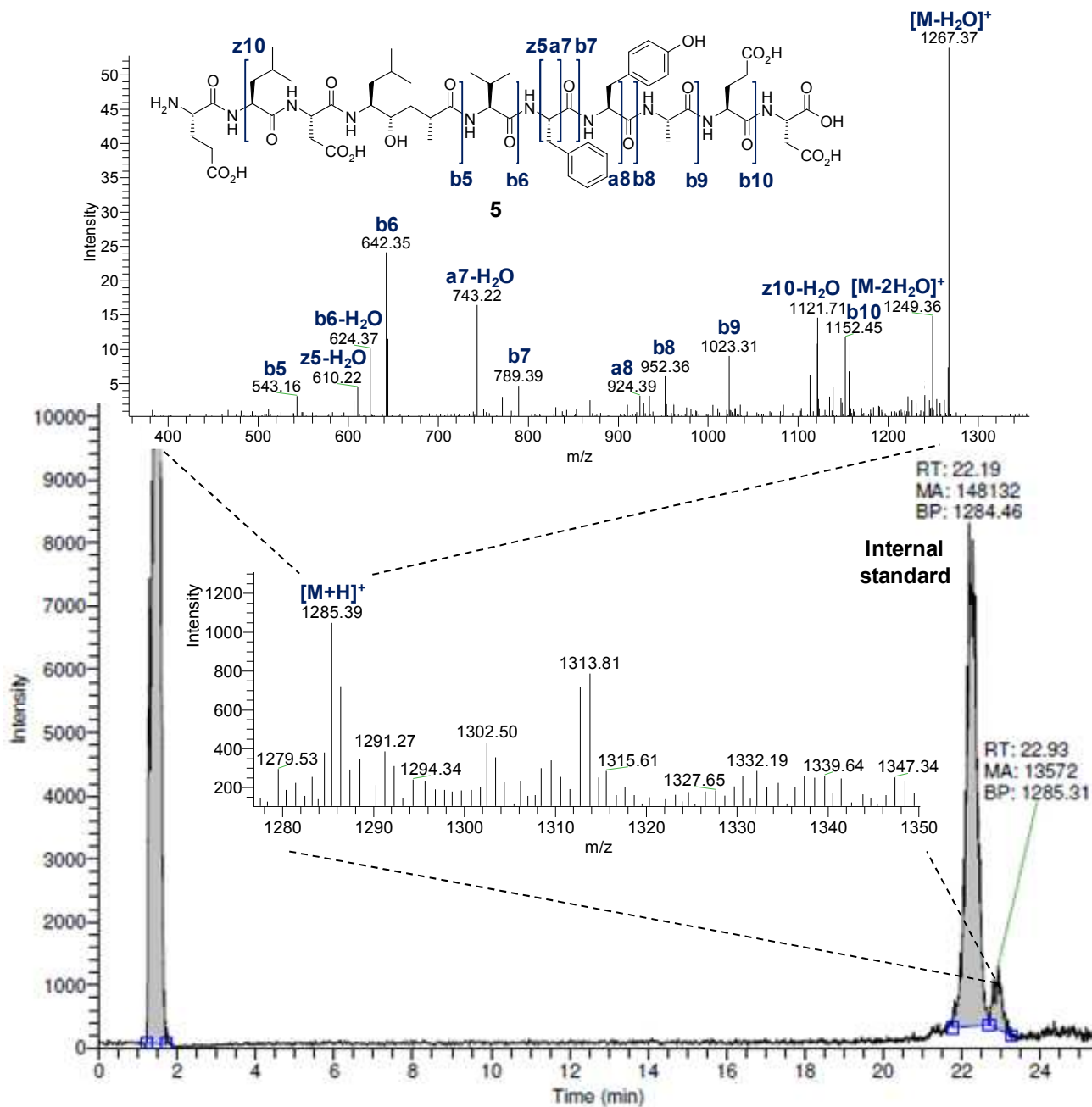


Figure 5:

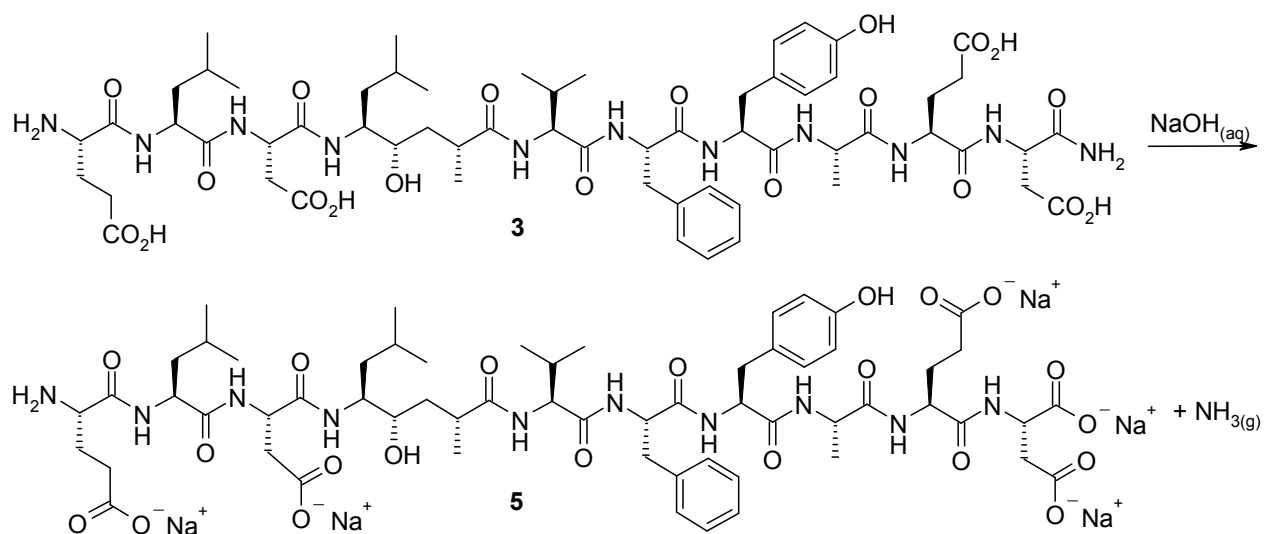


Figure 6:

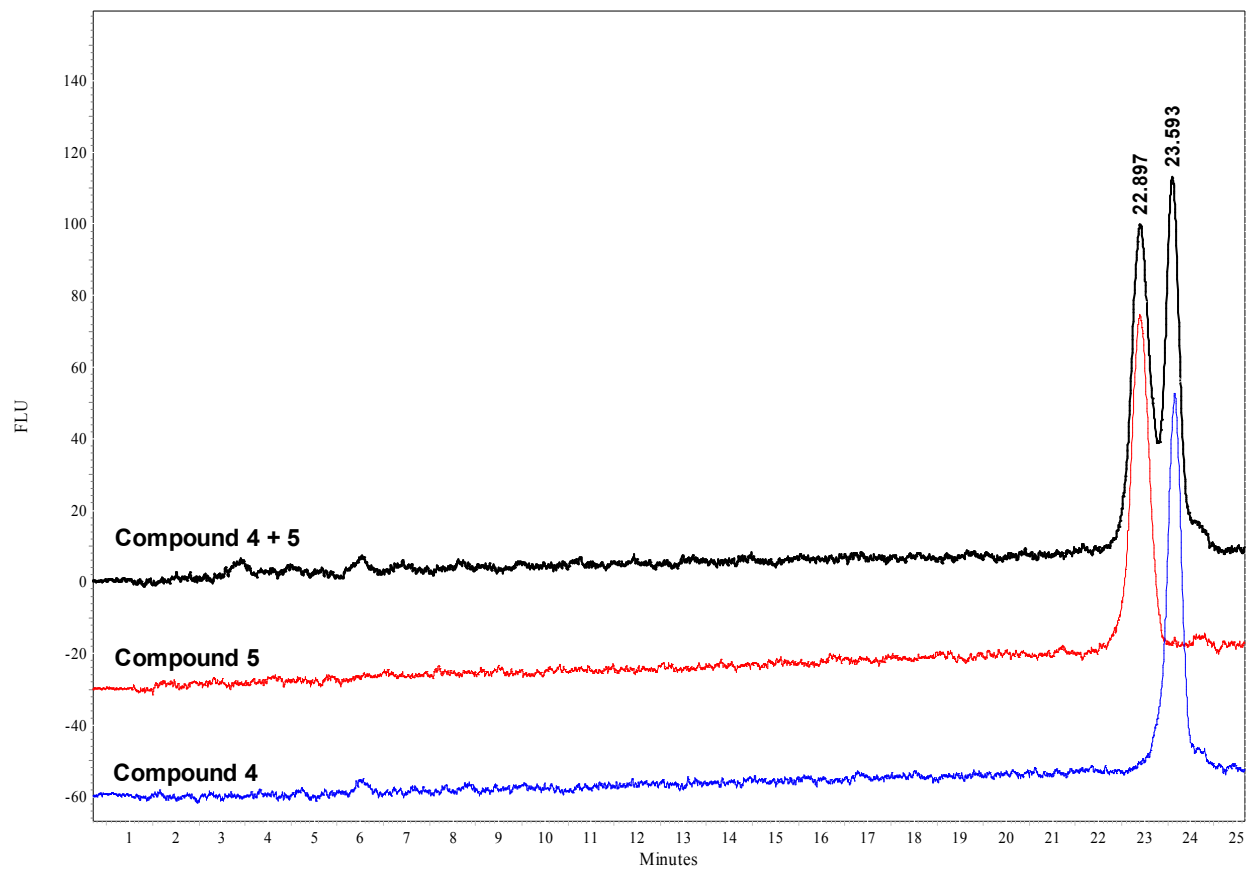


Figure 7:

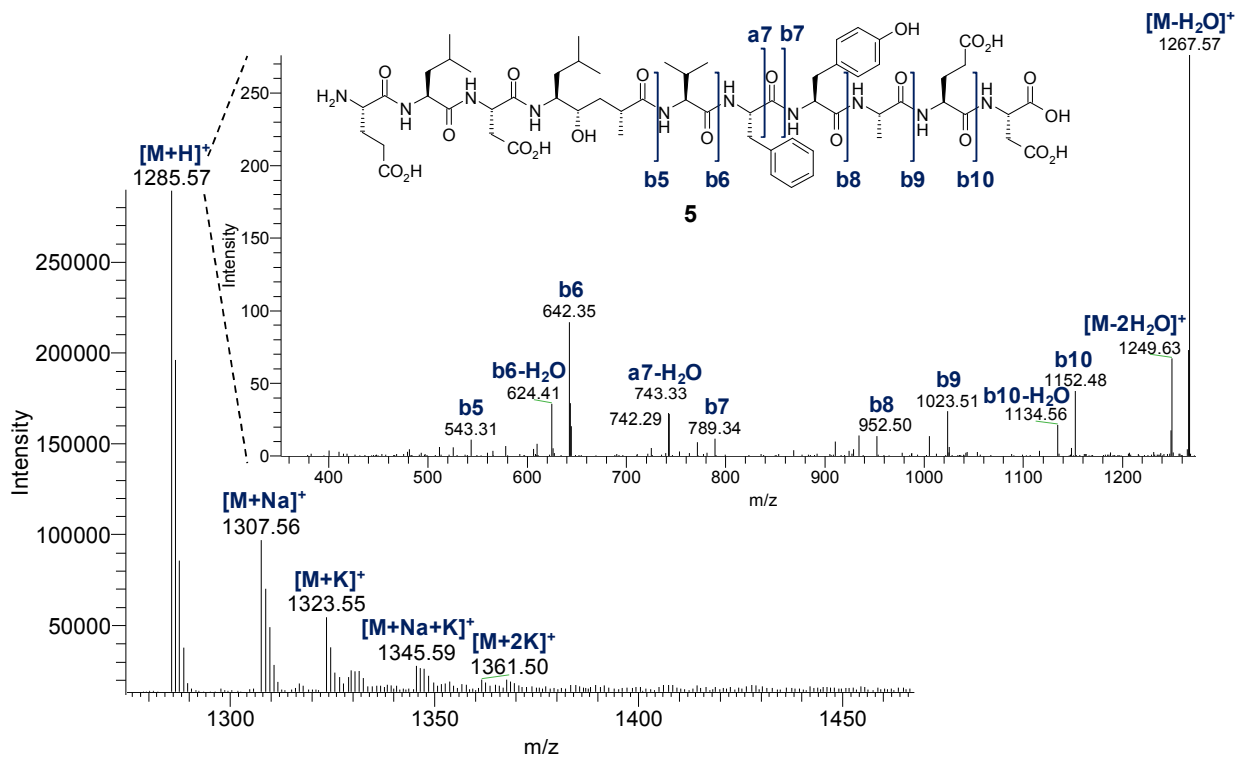


Figure 8:

**Supporting Information Available:** HPLC chromatograms of the pure compounds. This material is available free of charge via the Internet at <http://pubs.acs.org>.

## References

1. Stelzmann, R. A.; Norman Schnitzlein, H.; Reed Murtagh, F. An English translation of Alzheimer's 1907 paper, "Über eine eigenartige Erkrankung der Hirnrinde". *Clin. Anat.* **1995**, *8*, 429-431.
2. Citron, M, Alzheimer's disease: strategies for disease modification. *Nat. Rev. Drug Disc.* **2010**, *9*, 387-398.
3. Choi, S. H.; Kim, Y. H.; Hebisch, M.; Sliwinski, C.; Lee, S.; D'Avanzo, C.; Chen, H.; Hooli, B.; Asselin, C.; Muffat, J. A three-dimensional human neural cell culture model of Alzheimer's disease. *Nature* **2014**, <http://dx.doi.org/10.1038/nature13800> Oct 12.
4. John, V. Lead Target for Orchestrated Therapy of Alzheimer's Disease. *Wiley*; New Jersey, 2010; pp 15-29.
5. Hong, L.; Koelsch, G.; Lin, X.; Wu, S.; Terzyan, S.; Ghosh, A. K.; Zhang, X. C.; Tang, J. Structure of the protease domain of memapsin 2 ( $\beta$ -secretase) complexed with inhibitor. *Science* **2000**, *290*, 150-153.

- 1  
2  
3  
4  
5  
6  
7  
8  
9  
10  
11  
12  
13  
14  
15  
16  
17  
18  
19  
20  
21  
22  
23  
24  
25  
26  
27  
28  
29  
30  
31  
32  
33  
34  
35  
36  
37  
38  
39  
40  
41  
42  
43  
44  
45  
46  
47  
48  
49  
50  
51  
52  
53  
54  
55  
56  
57  
58  
59  
60  
6. Hong, L.; Turner, R. T.; Koelsch, G.; Shin, D.; Ghosh, A. K.; Tang, J. Crystal structure of memapsin 2 ( $\beta$ -secretase) in complex with an inhibitor OM00-3. *Biochemistry* **2002**, *41*, 10963-10967.
7. Shuto, D.; Kasai, S.; Kimura, T.; Liu, P.; Hidaka, K.; Hamada, T.; Shibakawa, S.; Hayashi, Y.; Hattori, C.; Szabo, B. KMI-008, a novel  $\beta$ -secretase inhibitor containing a hydroxymethylcarbonyl isostere as a transition-state mimic: design and synthesis of substrate-based octapeptides. *Bioorg. Med. Chem. Lett.* **2003**, *13*, 4273-4276.
8. Turner, R. T.; Koelsch, G.; Hong, L.; Castenheira, P.; Ghosh, A.; Tang, J. Subsite specificity of memapsin 2 ( $\beta$ -secretase): implications for inhibitor design. *Biochemistry* **2001**, *40*, 10001-10006.
9. Tang, J.; Ghosh, A. K.; Hong, L.; Koelsch, G.; Turner, R. T.; Chang, W. Study of memapsin 2 ( $\beta$ -secretase) and strategy of inhibitor design. *J. Mol. Neurosci.* **2003**, *20*, 299-304.
10. Butini, S.; Brogi, S.; Novellino, E.; Campiani, G.; K Ghosh, A.; Brindisi, M.; Gemma, S. The structural evolution of  $\beta$ -secretase inhibitors: a focus on the development of small-molecule inhibitors. *Curr. Top. Med. Chem.* **2013**, *13*, 1787-1807.
11. Abbott, N. J. Physiology of the blood-brain barrier and its consequences for drug transport to the brain. *Int. Congr.* **2005**, *1277*; 3-18.
12. Chang, W. P.; Koelsch, G.; Wong, S.; Downs, D.; Da, H.; Weerasena, V.; Gordon, B.; Devasamudram, T.; Bilcer, G.; Ghosh, A. K. In vivo inhibition of A $\beta$  production by memapsin 2 ( $\beta$ -secretase) inhibitors. *J. Neurochem.* **2004**, *89*, 1409-1416.

- 1  
2  
3  
4  
5  
6  
7  
8  
9  
10  
11  
12  
13  
14  
15  
16  
17  
18  
19  
20  
21  
22  
23  
24  
25  
26  
27  
28  
29  
30  
31  
32  
33  
34  
35  
36  
37  
38  
39  
40  
41  
42  
43  
44  
45  
46  
47  
48  
49  
50  
51  
52  
53  
54  
55  
56  
57  
58  
59  
60
13. Lefranc-Jullien, S.; Lisowski, V.; Hernandez, J. F.; Martinez, J.; Checler, F. Design and characterization of a new cell-permeant inhibitor of the  $\beta$ -secretase BACE1. *Br. J. Pharmacol.* **2005**, *145*, 228-235
14. Mackic, J.; Stins, M.; McComb, J.; Calero, M.; Ghiso, J.; Kim, K.; Yan, S.; Stern, D.; Schmidt, A.; Frangione, B. Human blood-brain barrier receptors for Alzheimer's amyloid-beta 1-40. Asymmetrical binding, endocytosis, and transcytosis at the apical side of brain microvascular endothelial cell monolayer. *J. Clin. Invest.* **1998**, *102*, 734.
15. Kim, S.-J.; Ahn, J.-W.; Kim, H.; Ha, H.-J.; Lee, S.-W.; Kim, H.-K.; Lee, S.; Hong, H.-S.; Kim, Y. H.; Choi, C. Y. Two  $\beta$ -strands of RAGE participate in the recognition and transport of amyloid- $\beta$  peptide across the blood brain barrier. *Biochem. Biophys. Res. Commun.* **2013**, *439*, 252-257.
16. Gospodarska, E.; Kupniewska-Kozak, A.; Goch, G.; Dadlez, M. Binding studies of truncated variants of the A $\beta$  peptide to the V-domain of the RAGE receptor reveal A $\beta$  residues responsible for binding. *Biochim. Biophys. Acta* **2011**, *1814*, 592-609.
17. Han, S.-H.; Kim, Y. H.; Mook-Jung, I. RAGE: the beneficial and deleterious effects by diverse mechanisms of actions. *Molecules and cells* **2011**, *31*, 91-97.
18. Takuma, K.; Fang, F.; Zhang, W.; Yan, S.; Fukuzaki, E.; Du, H.; Sosunov, A.; McKhann, G.; Funatsu, Y.; Nakamichi, N. RAGE-mediated signaling contributes to intraneuronal transport of amyloid- $\beta$  and neuronal dysfunction. *Proc. Natl. Acad. Sci.* **2009**, *106*, 20021-20026.

- 1  
2  
3  
4  
5  
6  
7  
8  
9  
10  
11  
12  
13  
14  
15  
16  
17  
18  
19  
20  
21  
22  
23  
24  
25  
26  
27  
28  
29  
30  
31  
32  
33  
34  
35  
36  
37  
38  
39  
40  
41  
42  
43  
44  
45  
46  
47  
48  
49  
50  
51  
52  
53  
54  
55  
56  
57  
58  
59  
60
19. Zlokovic, B. Can Blood–Brain Barrier Play a Role in the Development of Cerebral Amyloidosis and Alzheimer's Disease Pathology. *Neurobiol. Dis.* **1997**, *4*, 23-26.
20. Chen, Y.; Liu, L. Modern methods for delivery of drugs across the blood–brain barrier. *Adv. Drug Delivery Rev.* **2012**, *64*, 640-665
21. Ermolieff, J.; Loy, J. A.; Koelsch, G.; Tang, J. Proteolytic activation of recombinant pro-memapsin 2 (pro- $\beta$ -secretase) studied with new fluorogenic substrates. *Biochemistry* **2000**, *39*, 12450-12456.
22. Ghosh, A. K.; Shin, D.; Downs, D.; Koelsch, G.; Lin, X.; Ermolieff, J.; Tang, J. Design of potent inhibitors for human brain memapsin 2 ( $\beta$ -secretase). *J. Am. Chem. Soc.* **2000**, *122*, 3522-3523.
23. Turner, R. T.; Loy, J. A.; Nguyen, C.; Devasamudram, T.; Ghosh, A. K.; Koelsch, G.; Tang, J. Specificity of memapsin 1 and its implications on the design of memapsin 2 ( $\beta$ -secretase) inhibitor selectivity. *Biochemistry* **2002**, *41*, 8742-8746.
24. Casas, S.; Casini, P.; Piquer, S.; Altirriba, J.; Soty, M.; Cadavez, L.; Gomis, R.; Novials, A. BACE2 plays a role in the insulin receptor trafficking in pancreatic  $\beta$ -cells. *Am. J. Physiol.-Endoc. M.* **2010**, *299*, E1087-E1095.
25. Farzan, M.; Schnitzler, C. E.; Vasilieva, N.; Leung, D.; Choe, H. BACE2, a  $\beta$ -secretase homolog, cleaves at the  $\beta$  site and within the amyloid- $\beta$  region of the amyloid- $\beta$  precursor protein. *Proc. Natl. Acad. Sci.* **2000**, *97*, 9712-9717.
26. Reitz, A. B.; Choudhary, M. I. *Frontiers in Medicinal Chemistry. Bentham Science Publishers, Vol. 1*; Hilversum, 2004; 513-528.

- 1  
2  
3  
4  
5  
6  
7  
8  
9  
10  
11  
12  
13  
14  
15  
16  
17  
18  
19  
20  
21  
22  
23  
24  
25  
26  
27  
28  
29  
30  
31  
32  
33  
34  
35  
36  
37  
38  
39  
40  
41  
42  
43  
44  
45  
46  
47  
48  
49  
50  
51  
52  
53  
54  
55  
56  
57  
58  
59  
60
27. Benuck, M.; Marks, N. Differences in the degradation of hypothalamic releasing factors by rat and human serum. *Life Sci.* **1976**, *19*, 1271-1276.
28. Adessi, C.; Frossard, M.-J.; Boissard, C.; Fraga, S.; Bieler, S.; Ruckle, T.; Vilbois, F.; Robinson, S. M.; Mutter, M.; Banks, W. A. Pharmacological profiles of peptide drug candidates for the treatment of Alzheimer's disease. *J. Biol. Chem.* **2003**, *278*, 13905-13911.
29. Serra, A. T.; Poejo, J.; Matias, A. A.; Bronze, M. R.; Duarte, C. M. Evaluation of *Opuntia* spp. derived products as antiproliferative agents in human colon cancer cell line (HT29). *Food Res. Int.* **2013**, *54*, 892-901.
30. Niedermeyer, T. H.; Strohm, M. mMass as a software tool for the annotation of cyclic peptide tandem mass spectra. *PLoS One* **2012**, *7*, e44913.
31. Simplício, A. L.; Clancy, J. M.; Gilmer, J. F. Prodrugs for amines. *Molecules* **2008**, *13*, 519-547.
32. Wermuth, C. G. The practice of medicinal chemistry. *Academic Press*, 3rd ed; Burlington, 2011; pp 725-726.
33. Kauffman, F. C.; Frederick Kauffman, C.; Bock, K. W. Conjugation-deconjugation reactions in drug metabolism and toxicity. *Springer*, Berlin, 1994; pp 162-164.
34. Baumann, J.; von Bruchhausen, F.; Wurm, G. In vitro deacetylation studies of acetamidophenolic compounds in rat brain, liver and kidney. *Arzneim. Forsch.* **1983**, *34*, 1278-1282.

- 1  
2  
3  
4  
5  
6  
7  
8  
9  
10  
11  
12  
13  
14  
15  
16  
17  
18  
19  
20  
21  
22  
23  
24  
25  
26  
27  
28  
29  
30  
31  
32  
33  
34  
35  
36  
37  
38  
39  
40  
41  
42  
43  
44  
45  
46  
47  
48  
49  
50  
51  
52  
53  
54  
55  
56  
57  
58  
59  
60
35. Chan, W. C.; White, P. D. Fmoc solid phase peptide synthesis: A Practical Approach. *Oxford University Press*; New York, **2000**; pp 9-37.
36. Vila-Real, H.; Ventura, R.; Maycock, C.; Iranzo, O.; Simplicio, A. *unpublished results*.
37. Williams, J. W.; Morrison, J. F. [17] The kinetics of reversible tight-binding inhibition. *Methods in Enzymol.* **1979**, *63*, 437-467.
38. Kuzmič, P.; Sideris, S.; Cregar, L. M.; Elrod, K. C.; Rice, K. D.; Janc, J. W. High-throughput screening of enzyme inhibitors: automatic determination of tight-binding inhibition constants. *Anal. Biochem.* **2000**, *281*, 62-67.
39. Yung-Chi, C.; Prusoff, W. H. Relationship between the inhibition constant ( $K_i$ ) and the concentration of inhibitor which causes 50 per cent inhibition ( $I_{50}$ ) of an enzymatic reaction. *Biochem. Pharmacol.* **1973**, *22*, 3099-3108.
40. Henley, J. P.; Sadana, A. Deactivation theory. *Biotechnol. Bioeng.* **1986**, *28*, 1277-1285.

## Legends

Table 1: Molecular structure and inhibition potency of peptidomimetic BACE-1 inhibitors (mean value  $\pm$  standard deviation,  $n = 3$ ).

Figure 1: Rational drug design of **2**, starting from the BACE-1 inhibitor **1** and the RAGE ligand A $\beta$  18 – 23'. The **1** amino acid sequence was merged with A $\beta$  18 – 23' leading to an eleven amino acid peptidomimetic inhibitor, **2**.

Figure 2: Comparison of BACE-1 inhibition profiles by **1** ( $1.2 \pm 0.4$  nM) and **2** ( $2.0 \pm 0.1$  nM) (mean value  $\pm$  standard deviation,  $n = 3$ ).

Figure 3: Comparison between the inhibition profiles of BACE-1 and BACE-2, by **1**, **2**, **3** and **4** (mean value  $\pm$  standard deviation,  $n = 3$ ). The  $K_i^{app}{}_{BACE-2} / K_i{}_{BACE-1}$  ratio is 2.5 for **1**, 3.7 for **2**, 7.5 for **3** and 9.2 for **4**.

Figure 4: Metabolization profile of **1** ( $t_{1/2 \text{ serum}} = 2.2 \pm 0.5$ ;  $t_{1/2 \text{ brain}} = 5.8 \pm 0.7$ ), **3** ( $t_{1/2 \text{ serum}} = 2.1 \pm 0.1$ ;  $t_{1/2 \text{ brain}} = 2.3 \pm 0.1$ ), **4** ( $t_{1/2 \text{ serum}} = 6.0 \pm 0.2$ ;  $t_{1/2 \text{ brain}} = 3.43 \pm 0.1$ ) and **5** ( $t_{1/2 \text{ serum}} = 3.0 \pm 0.2$ ;  $t_{1/2 \text{ brain}} = 6.0 \pm 0.3$ ) (mean value  $\pm$  standard deviation,  $n = 3$ ).

Figure 5: LC-MS chromatogram and ESI-MS spectrum of the peak found in the chromatogram at 22.9 min in a brain sample, 1 hour after intravenous administration of **4** in

1  
2 mice; ESI-MS/MS spectrum of the peak 1285.39 amu and identification of the main peaks  
3  
4 found according to the expected metabolite, **5**.  
5  
6  
7

8  
9 Figure 6: Basic hydrolysis of **3** to afford **5**, with aqueous sodium hydroxide (500 mM) at  
10  
11 room temperature, overnight.  
12  
13

14  
15  
16 Figure 7: HPLC-FLU chromatograms of **4**, **5** and a mixture of both.  
17  
18  
19

20  
21 Figure 8: ESI-MS spectrum of the product of basic hydrolysis of **3** (found in the  
22  
23 chromatogram at 22.9 min); ESI-MS/MS spectrum of the main peak (1285.57 amu) and  
24  
25 identification of the main peaks found according to the expected product, **5**.  
26  
27  
28  
29  
30  
31  
32  
33  
34  
35  
36  
37  
38  
39  
40  
41  
42  
43  
44  
45  
46  
47  
48  
49  
50  
51  
52  
53  
54  
55  
56  
57  
58  
59  
60

## Table of Contents Graphic

